IEEE/CSC & ESAS European Superconductivity News Forum (ESNF), No. 6, October 2008
(ASC Preprint 2LPQ02 conforming to IEEE Policy on Electronic Dissemination, Section 8.1.9)

The published version of this manuscript appeared in *IEEE Transactions on Applied Superconductivity* **19**, No. 3, Part 2, 2403 - 2406 (2009)

Relation Between Transverse and Longitudinal Normal Zone Propagation Velocities in Impregnated MgB_2 Windings

Antti Stenvall, Risto Mikkonen, and Pavol Kováč

***Abstract*—The transverse normal zone propagation velocity, v_t, in impregnated magnets controls the 3D normal zone expansion during a quench. It is dominated by the thermal conductivities of the conductor insulation and the impregnation material. The longitudinal propagation velocity v_l is mainly determined by the heat generation, critical surface of the superdoncutor and thermal conduction along the conductor. It has been generally assumed that the ratio v_t/v_l is proportional to the the square root of the ratios of the corresponding effective heat conductivities. In this paper we study computationally the validity of this approach for an MgB_2 wire surrounded by an epoxy layer. We take into account the finite n-value of the composite conductor in our Finite Element Method (FEM) models. We computed v_l with Whetstone-Roos formula and 1D and 2D FEM models. The 2D model was also used to compute v_t. In addition to this, minimum quench energies given by the 1D and 2D FEM models were compared.**

***Index Terms*—finite element method, MgB_2, normal zone propagation velocity, simulation**

I. Introduction

TRANSVERSE normal zone propagation velocity v_t dominates the quench behaviour of an adiabatic superconducting magnet. It is largely dependent on the heat conductivity of the impregnation material and conductor insulation. The measurement of longitudinal normal zone propagation velocity v_l is essentially easier to measure than v_t, and also computation of it can be performed easily numerically or by utilizing some of the analytical formulae [1]–[3].

Some quench programs, such as Wilson's QUENCH [4, ch.9], utilize propagation velocities to compute the normal zone expansion in the winding. v_t can be approximated from v_l by applying the ratios of transverse and longitudinal heat conductivities λ_t and λ_l respectively as [4, p.208]

$$v_t \approx v_l \sqrt{\frac{\lambda_t}{\lambda_l}}. \tag{1}$$

Other analytical approaches exist too [5, p.353], whereas Finite Element Method (FEM) has been applied also earlier to solve v_t for an NbTi winding [6]. Term $\sqrt{\frac{\lambda_t}{\lambda_l}}$ is defined α and $\frac{v_t}{v_l} = \beta$. β depends largely on the coil filling factor, but for Nb-based conductors estimates between 0.1-0.01 have been presented [7].

Manuscript received August 18, 2008.

A. Stenvall and R. Mikkonen are with Tampere University of Technology, Electromagnetics, P.O. Box 692, FIN-33101 Tampere, Finland (phone: +385-3-3115 2080; fax: +358-3-3115 2160; e-mail: antti@stenvall.fi; www: http://www.tut.fi/smg).

P. Kováč is with Institute of Electrical Engineering, Slovak Academy of Sciences, Dúbravska cesta 9, 841 04 Bratislava, Slovakia.

By knowing β and v_l reliably, it is possible to use with enough accuracy a quench simulation program which utilises normal zone propagation velocities. This kind of programs are faster than quench simulation programs which discretise the winding and adopt, e.g., FEM of finite difference method [8]–[10].

In this paper we study computationally if α can be used to estimate β and derive v_t from v_l in MgB_2 windings with finite n-value. We derive v_l values from the Whetstone-Roos formula (W-R) [3] and 1D and 2D FEM models. For quench initiation in FEM models we compute the minimum quench energies (MQE) and ignit quenches with energies 10% higher than MQE. v_t values are also computed with 2D FEM model and derived from the v_l values by using α. We did computations with two n-values, 15 and 30.

II. Computational Model

Quench onset has been studied by solving the heat diffusion equation in transient conditions [11]–[13]. It has been noted that traditional closed form approaches are not applicable when solving mimimum quench energies of MgB_2 conductors [12]–[14]. This is especially due to finite n-values. We proposed a model for computing minimum propagation zones in [15] and adopted it to study also normal zone propagation velocities v_{NZP} in [16]. The results given by the model were also compared with measurements of multifilamentary MgB_2 wire with relatively good accuracy. Here we briefly review the model and present it in applicable form for computation of both minimum quench energies and v_{NZP}.

The basis of the model is to solve with FEM software the heat diffusion equation

$$\nabla \cdot \lambda \nabla T + Q + Q_{\text{ext}} = C_{\text{p}} \frac{\partial T}{\partial t}, \tag{2}$$

where, T, Q, Q_{ext} and C_{p} are the temperature, the Joule heat generation, the external heat generation and the volumetric specific heat, respectively.

In our approach, heat generation was computed according to the power-law as

$$Q = \frac{I}{A} \times \min \left\{ E_{\text{c}} \left(\frac{I}{I_{\text{c}}(B,T)} \right)^n, \rho_{\text{norm}}(T) \frac{I}{A} \right\} \tag{3}$$

where I, A, E_{c}, I_{c}, B and ρ_{norm} are the operation current, the conductor cross-sectional area, the electric field criterion (here 1 μV/cm), the critical current, the magnetic flux density and the conductor normal state resistivity, respectively. It is

important to note that this model includes current sharing because n-values are measured for entire conductors to characterize the current-voltage relation. Furthermore, it is not reasonable to use bulk, or single crystal, n-values to give $E-I$ relation for superconducting region of the conductor because then the extrinsic defects during the wire manufacturing are not included. These are, e.g., local variation of critical current density, sausaging and grain boundaries. After all, it has been discussed that conductor n-values arise from the local variation of cross-sectional critical currents [17].

External heat input can be computed in several ways. We used rectangular pulse with fixed duration and thus Q_{ext} was determined as

$$Q_{\text{ext}} = \begin{cases} 0 & \text{when } t < 0 \text{ or } t \geq t_{\text{dist}} \\ \frac{E_{\text{ext}}}{t_{\text{dist}}} & \text{when } 0 \leq t < t_{\text{dist}} \end{cases}, \tag{4}$$

where t_{dist} and E_{ext} are the disturbance duration and its energy, respectively. We had always $t_{\text{dist}} = 10$ ms.

Minimum quench energy E_{MQE} was determined as when $E_{\text{ext}} = E_{\text{MQE}}$ it states that

$$T\left(\text{Model's symmetry point}\right)|_{t=t_{\text{test}}} = T_{\text{cs}}, \tag{5}$$

where t_{test} is the test time used in the numerical algorithm and T_{cs} is the current sharing temperature which is derived as the inverse function of $I_{\text{c}}(T)$.

From the solved $T(t)$ distributions values of v_{NZP} were determined as

$$v_{\text{NZP}} = \frac{1}{N-1} \times \sum_{i=1}^{N-1} \frac{||\mathbf{x}_{i+1} - \mathbf{x}_i||}{t\left(T\left(\mathbf{x}_{i+1}\right) = T_{\text{cs}}\right) - t\left(T\left(\mathbf{x}_i\right) = T_{\text{cs}}\right)}, \tag{6}$$

where $\mathbf{x}_i$:s are points in the model. Fig. 1 shows schematically how we defined in the 1D FEM model v_{l} values. Also symmetry point for determination of MQE is shown. In Fig. 2 corresponding 2D model is shown with a view for determination of v_{t}.

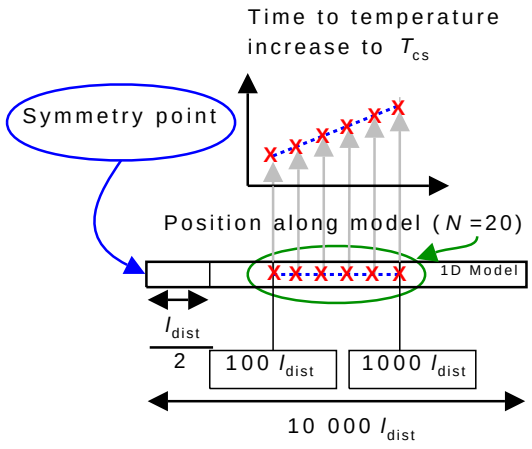

Fig. 1. Schematic view of 1D model for determining v_{NZP}. Length of disturbance l_{dist}=1 mm.

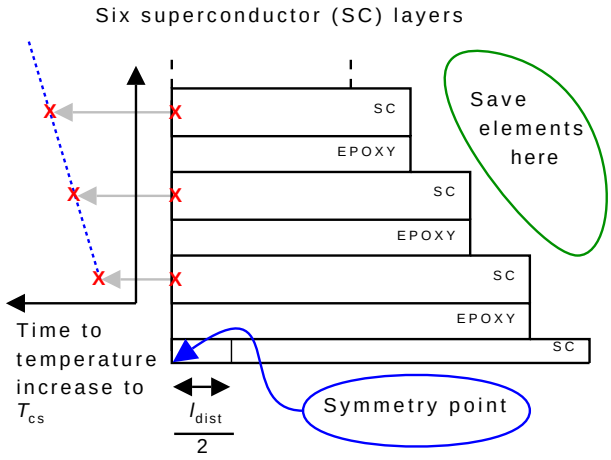

Fig. 2. Schematic view of 2D model for determining v_{t}.

Normal zone propagation velocities derived from the solutions were compared with W-R:

$$v_{\text{W-R}} = \frac{I}{A}\left[\frac{1}{\rho_{\text{norm}}\left(T_{\text{cs}}\right)\lambda_{\text{l}}\left(T_{\text{cs}}\right)} \times \left(C_{\text{p}}\left(T_{\text{cs}}\right) - \frac{1}{\lambda\left(T_{\text{cs}}\right)}\left.\frac{\text{d}\lambda}{\text{d}T}\right|_{T=T_{\text{cs}}} \int_{T_{\text{op}}}^{T_{\text{cs}}} C_{\text{p}}(T)\text{d}T\right) \times \int_{T_{\text{op}}}^{T_{\text{cs}}} C_{\text{p}}(T)\text{d}T\right]^{-\frac{1}{2}}, \tag{7}$$

where T_{op} is the operation temperature.

III. MgB_2 wire

The study was done with an MgB_2/Ti/Cu/Monel wire (Fig. 3) with volumetric fractions of 7% MgB_2, 14% Ti, 24% Cu and 55% Monel. Details of the conductor were given in [18].

Figure 4 presents critical current characteristics for investigated wire with selected values of magnetic flux density.

Material properties for the simulations were collected from the literature (see Table I). Not all the material properties were available and we used stainless-steel (SS) instead. RRR value of copper was expected to be 100. Effective material properties for the wire were computed according to the formulae given

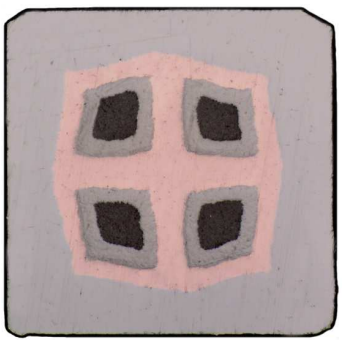

Fig. 3. MgB_2/Ti/Cu/Monel wire. Width and height are 1.2 mm.

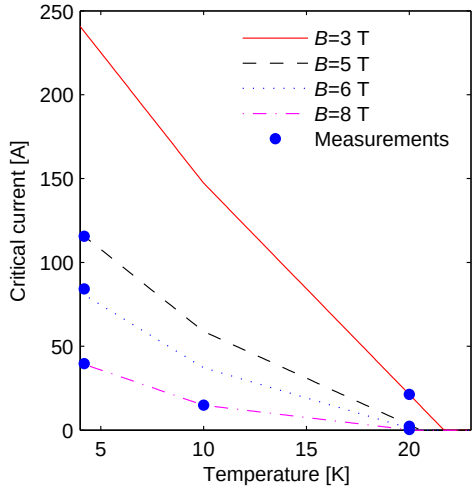

Fig. 4. Critical current characteristics for investigated wire.

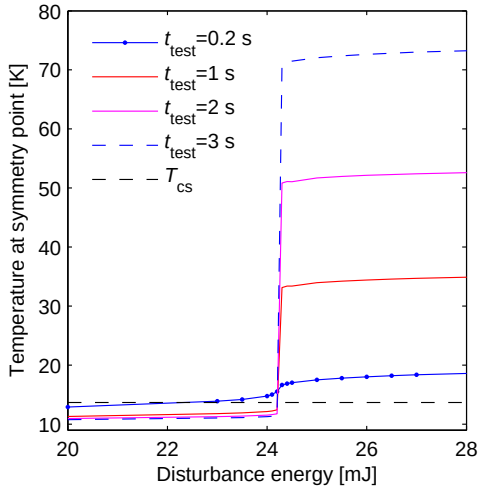

Fig. 5. Temperature at symmetry point as a function of disturbance energy for several values of t_{test} modelled with 1D FEM model. Also current sharing tempeture is shown.

TABLE I
REFERENCES FOR MATERIAL PROPERTIES. SS STATES DATA NOT FOUND, USED STAINLESS-STEEL INSTEAD.

Material	ρ	C_{p}	λ
MgB_2	[21]	[22]	[21]
Ti	SS [23, X-Z-4]	[23, VIII-O-3.1]	[24, 12-137]
Cu	[23, X-E-5]	[23, VIII-B-1]	[23, VII-B-2.1]
Monel	SS [23, X-Z-4]	SS [23, VIII-Q-7]	[23, VII-N-3,Drawn]
Epoxy	-	[23, VIII-N-1]	[25]

in [19]. For MgB_2 C_{p}, we expected porosity of 50% based on the studies presented in [20].

IV. RESULTS

We chose to study the presented wire at 10 K and 3 T. Then I_{c} was 147 A. In the 2D model we used epoxy thickness of 1 mm. We chose $t_{\text{test}} = 2$ s. Fig. 5 shows the modelled temperature at symmetry point at 10 K and 3 T as a function of disturbance energy for few times when $I = 0.7I_{\text{c}}$. Here 1D model was used. This shows that our choice was adequate. However, when n-value was 15 and I approached I_{c}, the sample warming was high enough and T_{cs} was reached before $t = 2$ s even without any disturbance in our 1D model. Due to this we stopped our simulations to $0.9I_{\text{c}}$.

For the starting point of the v_{l} analysis we needed to compute MQE (Fig. 6). Based on our earlier work, it was known that low n-values will result in higher MQE than high ones [15]. However, it is notable that the 2D FEM model gave considerably higher values for MQE than the 1D model. This hints that MQE measurements done for short-samples are very pessimistic when considering MQE of coils if they operate considerably below the critical current. For example at $0.5I_{\text{c}}$ and $n = 15$ 2D model gave sevenfold MQE. However, when I_{c} was approached the stabilisation given by the transverse heat conduction played smaller role. At $0.9I_{\text{c}}$ the sevenfold MQE diminished to twofold.

Fig. 7 presents the computed values of v_{l}. W-R agreed better with the results derived from the 1D model and with $n = 30$. However, the 2D model gave considerably lower

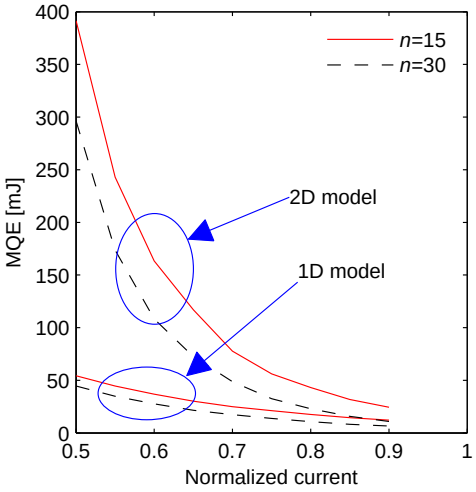

Fig. 6. Computed minimum quench energies at n-values of 15 and 30 with 1D and 2D FEM models.

propagation velocities than the 1D model and also when I_{c} was approached $v_{\text{W-R}}$ increased much more rapidly than the FEM models predicted. At $0.5I_{\text{c}}$ and $n = 30$ 1D model agreed best with W-R. Still the difference was 30% (5 cm/s). Corresponding difference in case of $n = 15$ was more than 40%. When $I = 0.9I_{\text{c}}$ the v_l values given by 1D model were 80% and 150% higher for n-values 30 and 15, respectively, than $v_{\text{W-R}}$.

When the differences in v_{l} were transferred to v_{t} by α, computed at T_{cs}, they remained almost constant as seen in Fig. 8. When we look at 2D model, α estimated β with good accuracy at low currents but when current reached $0.8I_{\text{c}}$ the error is already more than 50% and at $0.9I_{\text{c}}$ it is more than 100%.

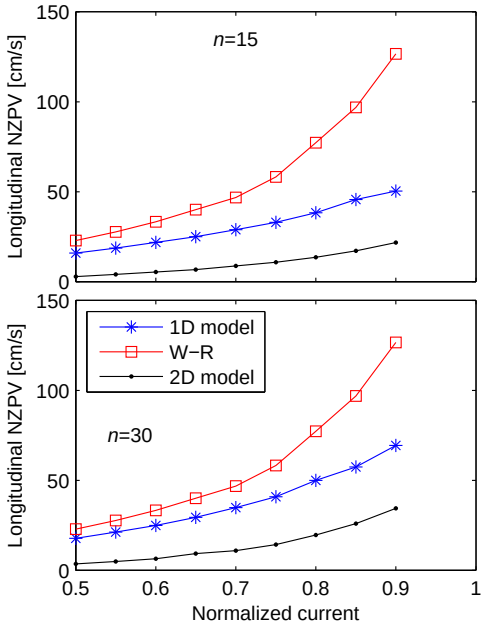

Fig. 7. Longitudinal normal zone propagation velocities.

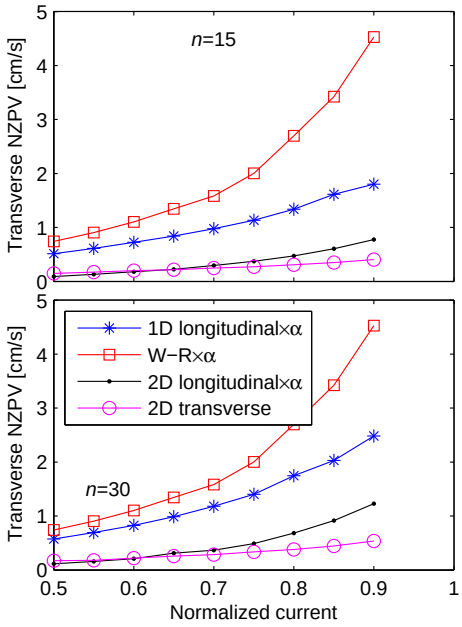

Fig. 8. Transverse normal zone propagation velocities.

V. Conclusions

We presented 1D and 2D models to compute longitudinal and transverse normal zone propagation velocities. We compared the results achieved with our models to the Whetstone-Roos formula and found the best agreement with 1D FEM model and W-R at low currents and high n-value. However, the correspondences of both 1D models with 2D FEM model were bad. This was seen also when MQE values were computed. It was also shown that in this particular case it is not adequate to estimate transverse normal zone propagation velocity from the longitudinal with the square root of the ratios of corresponding effective heat conductivities.

References

[1] A. Devred, "General formulas for the adiabatic propagation velocity of the normal zone", *IEEE Trans. Magn.*, vol. 25, pp. 1698-1705, 1989.

[2] H. H. J. ten Kate, H. Boschman, and L. J. M. van de Klundert, "Longitudinal propagation velocity of the normal zone in superconducting wires", *IEEE Trans. Magn.*, vol. 23, pp. 1557-1560, 1987.

[3] C. N. Whetstone, and C. E. Roos, "Thermal phase transitions in superconducting Nb-Zr alloys", *J. Appl. Phys.*, vol. 36, pp. 783-791, 1965.

[4] M. N. Wilson, "Superconducting Magnets", Oxford: Oxford University Press, 1983.

[5] Y. Iwasa, "Case Studies in Superconducting Magnets", New York: Plenum Press, 1994.

[6] A. Ishiyama, H. Matsumura, W. Takita, and Y. Iwasa, "Quench propagation analysis in adiabatic superconducting windings", *IEEE Trans. Magn.*, vol. 27, pp. 2092-2095, 1991.

[7] R. Mikkonen, A. Korpela, J. Lehtonen, J. Paasi, and J. Vuorinen, "Design of a 0.2 MJ conduction cooled Nb_3Sn SMES system", *IEEE Trans. Appl. Supercond.*, vol. 10, pp. 784-787, 2000.

[8] V. Picaud, P. Hiebel, and J-M. Kauffmann, "Superconducting coils quench simulation, the Wilson's method revisited", *IEEE Trans. Magn.*, vol. 38, pp. 1253-1256, 2002.

[9] A. Stenvall, A. Korpela, R. Mikkonen, and G. Grasso, "Quench analysis of MgB_2 coils with a ferromagnetic matrix" *Supercond. Sci. Technol.*, vol. 19, pp. 581-588, 2006.

[10] R. Yamada, E. Marscin, A. Lee, M. Wake, and J-M. Rey, "3-D/2-D quench simulation using ANSYS for epoxy impregnated Nb_3Sn high magnetic field magnets", *IEEE Trans. Appl. Supercond.*, vol. 13, pp. 1696-1699, 2003.

[11] K. Ishibashi, M. Wake, M. Kobayashi, and A. Katase, "Thermal stability of high current density magnets", *Cryogenics*, vol. 19, pp. 633-638, 1979.

[12] E. Martínez, F. Lera, M. Martínez-López, Y. Yang, S. I. Schlachter, P. Lezza, and P. Kováč, "Quench development and propagation in metal/MgB_2 conductors", *Supercond. Sci. Technol.*, vol. 19, pp. 143-150, 2006.

[13] E. Martínez, E. A. Young, M. Bianchetti, O. Munoz, S. I. Schlachter, and Y. Yang, "Quench onset and propagation in Cu-stabilized multifilament MgB_2 conductors", *Supercond. Sci. Technol.*, vol. 21, 025009 (8p), 2008.

[14] H. van Weeren, "Magnesium Diboride Superconductors for Magnet Applications", PhD Thesis, University of Twente, The Netherlands, 2007.

[15] A. Stenvall, A. Korpela, J. Lehtonen and R. Mikkonen, "Formulation for 1D minimum propagation zone", *Physica C*, vol. 468, pp. 968-973, 2008.

[16] A. Stenvall, and R. Mikkonen, "Thermal transients in MgB_2 conductors", *In press, To appear in MgB_2 Superconductor Research* (Nova Publishers), 2008.

[17] H. S. Edelman, and D. C. Larbalestier, "Resistive transitions and the origin of the n value in superconductors with a Gaussian critical-current distribution", *J. Appl. Phys.*, vol. 74, pp. 3312-3315, 1993.

[18] P. Kováč, I. Hušek, T. Melišek, and T. Holúbek, "Properties of stabilized MgB_2 composite wire with Ti barrier", *Supercond. Sci. Technol.*, vol. 20, pp. 771-776, 2008.

[19] A. Stenvall, A. Korpela, R. Mikkonen, and G. Grasso, "Stability considerations of multifilamentary MgB_2 tape", *Supercond. Sci. Technol.*, vol. 19, pp. 184-189, 2006.

[20] C. F. Liu, G. Yan, S. J. Du, W. Xi, Y. Feng, P. X. Zhang, X. Z. Wu, and L. Zhou, "Effect of heat-treatment temperatures on density and porosity in MgB_2 superconductor", *Physica C*, vol. 386, pp. 603-606, 2003.

[21] M. Schneider, D. Lipp, A. Gladun, P. Zahn, A. Handstein, G. Fuchs, S-L. Drechsler, M. Richeter, K-H. Müller, and H. Rosner, "Heat and charge transport properties of MgB_2", *Physica C*, vol. 363, pp. 6-12, 2001.

[22] Ch. Wälti, E. Felder, C. Degen, G. Wigger, R. Monnier, B. Delley, and H. R. Ott, "Strong electron-phonon coupling in superconducting MgB_2: A specific heat study", *Phys. Rev. B*, vol. 64, 172515 (4p), 2001.

[23] J. E. Jensen, W. A. Tuttle, R. B. Stewart, H. Brechna, and A.G. Prodell (editors), "Selected Cryogenic Data Notebook", Brookhaven National Laboratory, 1981.

[24] D. R. Lide (Editor-in-Chief), "Handbook of Chemistry and Physics 74th edition 1993-1994", Boca Raton: CRC Press, 1993.

[25] J. Lehtonen, R. Mikkonen, and J. Paasi, "Effective thermal conductivity in HTS coils", *Cryogenics*, vol. 40, pp. 245-249, 2000.